Lab-on-a-Bead: Polymeric Natural Deep Eutectic Solvents as a Versatile Platform for (Bio)sensor Design

Federico J. V. Gomez,[1] Ezequiel Vidal,[2,3] Graciela Zanini,[2] Claudia E. Domini,[2] Maria Fernanda Silva,[1] and Carlos D. Garcia[3*]

[1]Instituto de Biología Agrícola de Mendoza (IBAM-CONICET), Facultad de Ciencias Agrarias, Universidad Nacional de Cuyo, Mendoza, Argentina

[2]INQUISUR, Departamento de Química, Universidad Nacional del Sur (UNS)-CONICET, Bahía Blanca, Argentina

[3]Department of Chemistry, Clemson University, Clemson SC 29634, USA

[*] To whom correspondence should be addressed. 211 S. Palmetto Blvd, Clemson, SC, 29634, United States, e-mail: cdgarci@clemson.edu

Abstract

Natural polymers offer not only low-cost, wide availability, biocompatibility, and biodegradability but also a rich chemical functionality towards custom modifications and new applications. Among those, sodium alginate (ALG) offers a number of competitive advantages, including the possibility to form beads by a simple process call spherification as well as their modification by a wide number of processes, including the possibility to mixing the alginate solution with deep eutectic solvents (DES). Thus, and considering the capacity of DES to stabilize enzymes, the main objective of this work was to design and fabricate a new PODES (using ALG as one of the components, ALG_{PODES}) and to deploy this material as a new phase to develop colorimetric biosensors. The formed beads displayed a narrow size distribution (2.9 ± 0.1 mm) and a permeable structure with large internal cavities (25-100 μm). The applicability of these beads towards analytical applications (*lab-on-a-bead*) was demonstrated by integrating three sensing platforms and by their application in real food samples.

1. INTRODUCTION

The last few decades have witnessed a significant push to replace synthetic polymers for biodegradable natural polymers.[1] Natural polymers composed of polysaccharides (cellulose, chitosan, alginate, etc.) or proteins (silk, fibroin, gelation) offer not only low-cost, wide availability, biocompatibility, and biodegradability but also a rich chemical functionality towards custom modifications and new applications.[2] Among those, and although cellulose[3, 4] and chitosan[5] are probably the most used biopolymers towards the development of analytical applications, sodium alginate (ALG) offers a number of competitive advantages. ALG is a linear anionic biopolymer extracted from brown algae, composed by β-D-mannuronate (M) and α-L-guluronate (G) units linked by β-1,4 and α-1,4 glycosidic bonds. Perhaps the most notable property of ALG is that paired guluronic units are able to accommodate divalent ions (*e.g.*, calcium, copper, strontium, barium, etc.), enabling the formation of hydrogel beads, with few mm in diameter[6-8] and large internal pores (150-400 μm).[9, 10] While the application of these porous beads in the food,[11, 12] biomedical,[9, 13, 14] or pharmaceutical[15, 16] industries is already established, several groups have recently explored the possibility to used them as sorbents materials for solid phase extraction.[7, 17-19] An even less explored field is the possibility to use alginate beads as a biosensing platform.[17, 20-22] The main problem limiting this application is that although the porous structure of the material allows proteins[21, 23] and other components to adsorb on (or penetrate into) the beads, these water-soluble molecules can also be released by either simple diffusion or triggered by the sample matrix (pH changes, ionic strength, etc.).[13, 24]

Aiming to control the kinetics of the release process, several approaches have been proposed including adjusting the concentration of the components,[25] adding sorbent particles,[6, 7, 20] encapsulating the beads within hydrophobic materials (wax),[26] forming composites with other polymers,[27-29] and modifying the native functional groups (-OH and -COOH) of the alginate.[9, 14, 30-33] In addition, and albeit not targeting biosensing applications, a few groups have recently reported the possibility to synthetize beads mixing the alginate solution with deep eutectic solvents (DES).[19, 34-36] These DES (mixtures of two or more pure compounds for which the eutectic temperature is below that of the ideal liquid mixture)[37-39] can not only be made with natural molecules (acids, sugars, alcohols, etc.) but can also open the door to unique modifications (polarity, vapor pressure, viscosity, etc.) to the system.[40, 41] In this sense, polymeric deep eutectic solvents, also known as PODES, are a new and interesting family of materials that combine

characteristics from polymers with the traditional advantages of DES,[42, 43] enabling the formation of a stable phase supported by the hydrogen-bond network.[38, 44]

Thus, and considering the capacity of DES to stabilize enzymes,[45-48] the main objective of this work was to design and fabricate a new PODES using ALG as one of the components (ALG_{PODES}). The hypothesis behind the project was that the new ALG_{PODES} would enable the formation of beads. This stable network would in turn, provide a new phase to preserve the activity of the biorecognition elements and retain other molecules of interest (chromogenic agents), thus supporting their use towards the development of colorimetric biosensors. To demonstrate the feasibility of the proposed approach, a new PODES (composed of alginate, glycerol, and water; referred to as ALG_{PODES}) was developed and then used to form beads (in the presence of calcium ions), which were then morphologically characterized and compared against ALG beads in terms of their capacity to retain the selected redox indicators and stabilize the selected enzymes. The suitability of the ALG_{PODES} beads towards the development of colorimetric sensors for glucose, lactate and glutamate was also assessed and its applicability demonstrated with real food samples (oyster and soy sauces). We believe this platform (*lab-on-a-bead*) provides a new analytical paradigm, where a handful of beads (sensors) can be added to a sample; instead of adding the sample to the sensor.

2. MATERIALS AND METHODS

2.1 Chemicals. Glucose oxidase (from *Aspergillus niger*, 17300 U g^{-1}, GOx), peroxidase type II (from horseradish 156 U mg^{-1}; HRP), lactate oxidase (from *Pediococcus* sp., 20 U mg^{-1}; LOx), L-glutamate oxidase (from *Streptomyces* sp., 5 U mg^{-1}; GlutOx), D-(+)-glucose, sodium L-lactate, sodium 3,5-dichloro-2-hydroxybenzenesulfonic acid (DHBS), L-glutamic acid, and 3,3',5,5'-tetramethylbenzidine ≥98% (TMB) were purchased from Sigma-Aldrich (St. Louis, MO). 4-Aminoantipyrine (AAP) was obtained from Alfa Aesar (Ward Hill, MA). Calcium chloride was purchased from E.M. Science (Gibbstown, NJ). Sodium phosphate monobasic anhydrous and sodium phosphate dibasic anhydrous were received from Fisher Scientific (Waltham, MA). o-Dianisidine dihydrochloride (ODI) ≥98% was obtained from Tokyo Chemical Industry (Portland, OR). All chemicals were used as received and solutions were prepared in ultrapure water (18 MΩ.cm, Barnstead Nanopure; Dubuque, IA) or methanol. For the analysis, stock solutions of each analyte (25 mmol L^{-1} lactate, 20 mmol L^{-1} glucose, and 20

mmol L^{-1} glutamate) were prepared in 100 mmol L^{-1} PBS (pH = 7.0) and then diluted with PBS at different ratios to cover the concentration ranges utilized in the calibration curves.

2.2 Enzymatic solutions and chromogenic agents. For the glucose assay, a 1:5 mixture of HRP (339 U mL^{-1}, in 100 mmol L^{-1} PBS pH=7.0) and GOx (645 U mL^{-1}, in 100 mmol L^{-1} PBS pH=7.0) was first prepared. The corresponding chromogenic agent (ODI) was prepared in 100 mmol L^{-1} PBS (pH=6.0) to a final concentration of 10 mmol L^{-1}. For lactate detection, a 1:1 mixture of LOx (100 U mL^{-1}, in 100 mmol L^{-1} PBS pH = 7.0) and HRP (339 U mL^{-1}, in 100 mmol L^{-1} PBS pH = 6.0) was prepared. In this case, 4-AAP (6.6 mmol L^{-1}) and DHBS (6.6 mmol L^{-1}) were dissolved in 100 mmol L^{-1} PBS (pH = 6.0) and kept in the fridge covered with aluminum foil to protect them from light. For the glutamate assay, a 1:1 mixture of GlutOx (4.16 U mL^{-1}, in 100 mmol L^{-1} PBS pH = 7.0) and HRP (339 UmL^{-1}, in 100 mmol L^{-1} PBS pH = 7.0) was prepared. In this case, TMB (selected as the chromogenic agent[49]) was dissolved in MeOH (15 mmol L^{-1}) and kept in the fridge covered in aluminum foil to protect it from light). It is also important to note that although specific pairs of enzymes and chromogenic agents were selected (GOx/HRP-ODI, LOx/HRP-AAP/DHBS, and GlutOx/HRP-TMB), they can be interchanged to fit specific demands.

2.3 ALG_{PODES} preparation and beads formation. ALG_{PODES} were prepared following the classical heating and stirring method, considering the chemical similarities between the alginate monomers and glucose (that readily forms NADES[39, 50, 51]). It is important to state that the process results in the formation of a new phase (rather than a simple mixture of the components[52-54]) supported by hydrogen-bonding and that is preserved even after dilution.[38, 44]

For this purpose, the components were placed in a 20 mL, capped transparent vial, and heated at 60°C during 3 hr with constant stirring (350 rpm). Preliminary experiments explored the suitability of several components and molar ratios to form stable ALG_{PODES} (that remained as a clear liquid at room temperature for at least one week), allowing the selection of a mixture composed of glycerol:alginate:water (5:1:15 molar ratio), as the optimum system. To lower its viscosity and facilitate the extrusion process, the ALG_{PODES} (at room temperature) was first diluted with water (1:1 w/w). Next, the ALG_{PODES} was mixed with a solution containing the selected enzymes and chromogenic agents in

a proportion of 1:1 (w/w), leading to a system containing a final concentration of 5% ALG. Control beads were developed using the same procedure but from stock solutions containing either 2% or 10% ALG, which were mixed with a solution containing the selected enzymes and chromogenic agents in a proportion of 1:1 (w/v), leading to extrusion solutions containing 1% ALG or 5% ALG, respectively. These solutions were used to prepare beads via the extrusion-dripping method, from a syringe fitted with a 21G needle (BD PrecisionGlide) and into a glass vial containing 5 mL of a solution of 0.1 M $CaCl_2$ under gentle stirring (300 rpm). The obtained beads were left in the $CaCl_2$ solution for 10 min to complete the cross-linking process, rinsed several times with distilled water to remove any excess of $CaCl_2$ from their surface, strained (to remove any excess of water), and stored in a glass vial until use.

2.4 Image capture and processing. The image capture was made using a REDMI Note 10s smartphone built-in camera. The settings were configured using the manual mode adjusting the white balance to cloudy mode, focus to 1.79 mm, shutter speed in 1/200 seconds, and ISO 80. For short distance captures the Macro lens was used with a resolution of 2 megapixels. For dynamic experiments, the time-lapse function was used, capturing pictures every 5 seconds for 600 seconds. An *ad-hoc* Plexiglas® cell (Figure SI 1) was designed using Corel Draw software, and fabricated using an Epilog Mini Laser Engraver, equipped with a 30 W CO_2 laser (85% power, 15% speed).[55] In addition, an *ad-hoc* stand made of black plexiglass was used to isolate the device from ambient light and to set the capture distance between the camera and the beads to 35mm. Back illumination was obtained using a USB-powered LED light bar (Extreme Tech). The free software ImageJ[56] 1.51q was used for the edition and processing of the images. Both still and time-lapse images were processed as stacks using the same procedure, to increase the reproducibility. The region of interest (ROI) selected in each capture was set as the circular area of each individual bead. Size distribution studies were performed by measuring the diameter of the different beads in those pictures, using the Set Scale function calibrated scale as a reference.

All images were obtained in RGB mode and preliminary studies allowed selecting the blue channel for ODI and the green channel both for AAP/DHBS and TMB. Under these conditions, the best sensitivity and selectivity was obtained.

2.5 Scanning Electron Microscopy. Micrographs were obtained using a Hitachi SU6600 Scanning Electron Microscope. Beads fabricated using 1% ALG, 5% ALG, or the proposed ALG_{PODES} (diluted and containing the enzyme/dyes) were freeze dried during 24 hs using a LabConco FreeZone 4.5 Liter Freeze Dry System (Kansas City, MO). This method was selected to preserve (as much as possible) the structure of the beads.

2.6 Real samples. Four soy-based sauces (soy sauce, orange sauce, low-sodium soy sauce and teriyaki sauce; Great Value) and one oyster-flavored sauce (Lee Kum Kee) were obtained from a local market. Prior to their analysis, sauces were diluted 25-fold with distilled water and then placed into the sample reservoirs for analysis. All samples were maintained at room temperature.

3. RESULTS AND DISCUSSION

3.1 Beads morphology and size. To determine the morphology and the inner structure of the ALG_{PODES} beads, SEM measurements were performed. For this purpose, plain and split beads were deposited onto carbon tape, and placed in the microscope. SEM micrographs show that ALG_{PODES} beads feature a rather homogeneous external surface (shell-like, Figure 1A) with small pores (~100 nm) that would allow analytes to permeate. In contrast, the inside of the beads showed a layered structure, leading to the formation of large internal cavities (25-100 μm), as it can be seen in Figure 1B. This internal foam-like structure is common to the other Ca-alginate beads investigated (formed using either 1% ALG, Figure SI 2 or 5% ALG, Figure SI 3) as well as to those reported in the literature.[10, 36, 57-59] It is relevant to mention the work from Voo *et al*,[25] who reported that beads formed with 100 mg/mL ALG also displayed a layered structure, effect that was attributed to the coalescence of the partially-gelled Ca-alginate, trapped within the highly-crosslinked shell.

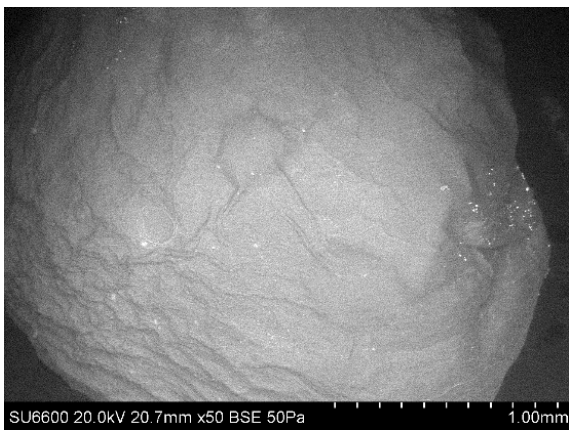

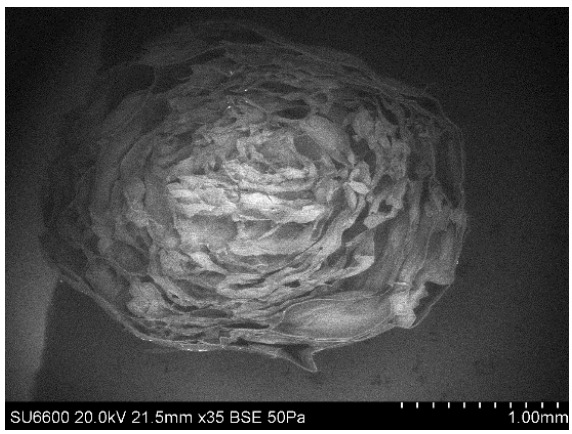

Figure 1: SEM images obtained with ALG$_{PODES}$ beads upon freeze-drying for 24hs.

Additionally, optical images collected from as-prepared beads (Figure SI 4) showed the expected[53, 60] spherical shape with a glossy, homogeneous, and smooth surface; indicating the compatibility of the new ALG$_{PODES}$ with established spherification processes.[61] The size distribution of the selected beads (1% ALG, 5% ALG, or ALG$_{PODES}$) was also investigated. For that purpose, 300 beads of each composition were photographed, and their diameter measured using ImageJ software. As it can be observed in Figure 2, beads formed with 1% ALG displayed the smallest size, with a diameter of 2.2 ± 0.3 mm and the beads formed with 5% ALG showed a diameter of 3.4 ± 0.2 mm. These dimensions are in agreement with previously reported values for ALG beads produced under various experimental conditions (including the size dependence with respect to the concentration of the polymer),[61, 62] although beads covering a much wider range (20 µm to 7 mm)[63] have been reported. ALG$_{PODES}$ beads presented a narrower size distribution, featuring an average diameter of 2.9 ± 0.1 mm (ranging from 2.4 mm to 3.2 mm), matching other reports[53] and showing a significant difference with respect to the ALG control beads. This difference can be attributed to the decreased surface tension of the ALG$_{PODES}$ (with respect to the 5% ALG), due to the presence of glycerol in the dripping solution that has a dominant effect on the size of the droplet released from the needle.[61, 62]

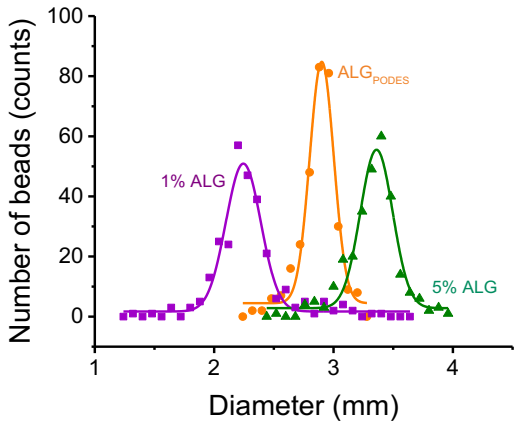

Figure 2: Size distribution of the selected beads (1% ALG, 5% ALG, or ALG$_{PODES}$). 300 beads of each composition were photographed, and their diameter measured using ImageJ software.

3.2 Stability of the system. Determining and preserving the catalytic activity of the ensemble (enzymes + chromogenic agents) is essential to deploy the ALG$_{PODES}$ beads as a sensing platform**.** Thus, and considering that NADES can enhance solubility and stability of several macromolecules,[64, 65] the stability

of the sensors was assessed considering the activity of GOx as well as the retention of the redox dyes inside the selected beads.

In the first case, the enzymatic activity of GOx/HRP (as model enzyme for the development of biosensors[66]) was measured and analyzed as a function of time. For these experiments, 1% ALG, 5% ALG, and ALG_{PODES} beads were prepared containing the combination of GOx/HRP-ODI as a model reporter and maintained at room temperature during the period of the experiment. These conditions were specifically selected to challenge the stability of the enzyme, considering that lower temperatures would extend the lifetime of the sensor[67] and that the selected redox dye (ODI) would remain within the beads (*vide infra*). Thus, at the selected times, three beads of each composition were placed into the Plexiglas® cell (Figure SI 1) containing 1 mL of a 0.1 mM glucose solution and their color development followed, capturing pictures every 5 seconds for 600 seconds. While only the average color intensity of the beads at 600 seconds was used for the herein described analysis, this procedure was adopted for all experiments to ensure consistency. As it can be observed in Figure 3, all the beads showed catalytic activity when exposed to glucose, confirming the accessibility of the enzymes through the pores in the external shell of the beads (Figure 1A). As it can also be observed in Figure 3, the highest response was obtained for the ALG_{PODES} beads, followed by the bead synthetized from 5% ALG and then those made from 1% ALG. As all these beads contain the same amount of GOx/HRP-ODI, these initial results would support the idea that the ALG_{PODES} provide a more favorable environment for the reaction.

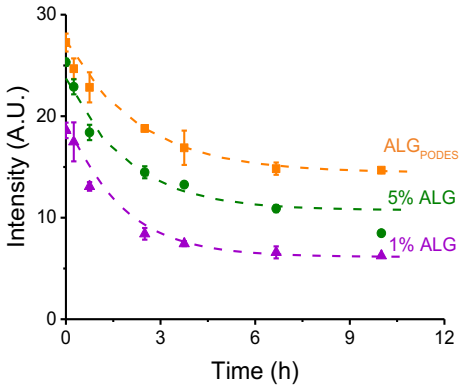

Figure 3: Stability of the system (enzymes). 1% ALG (purple), ALG_{PODES} (orange) and 5% ALG (green). Alginates were mixed with solutions containing o-Di dye and the mixture of enzymes (GOx and HRP) in order to reach the appropriate final concentration. Beads were prepared dropping the appropriate alginate solution into 5 mL of $CaCl_2$ 0.1 M under constant magnetic stirring. Beads were submerged in 1 mL of glucose 0.1 mM.

These experiments also displayed a gradual decrease in the colorimetric response of the beads, that stabilized approximately 4 hours after the preparation. While the ALG_{PODES} beads showed a decrease of 40 ± 3 % in the response (after 10 hours at room temperature), the color development decreased by 65 ± 2 % and by 67 ± 3 %, when beads composed of 5% ALG or 1% ALG were used. We hypothesize that these changes, which are somewhat in agreement with previous reports,[68-70] could be attributed to slight conformational changes in the enzymes, induced by the ALG_{PODES} (or ALG) matrix,[71-74] that surrounds the proteins and (upon stabilization) creates a microenvironment that maintains their conformation and protects their active sites.[75] Considering that no color development was observed outside the beads, the release of the enzymes[76, 77] or the redox dye to the solution is unlikely to be significant contributor to the decrease within the investigated timescale. Based on these results, ALG_{PODES} were considered a superior platform for the development of the proposed biosensor and thus, used for the remaining experiments.

Besides retaining the enzymatic activity, it is critical to consider that dyes and small molecules can easily penetrate into (or scape from) the alginate beads due to their inherent porous structure.[78] Therefore, the ability of the beads to retain the selected redox dyes was evaluated over time, considering the color development within the beads (functionality) as well as in the area surrounding the beads (leaching), upon exposure to the solution containing the analyte. For these experiments, 1% ALG, 5% ALG, and ALG_{PODES} beads were prepared with GOx/HRP (as a model reporter) but containing each of the selected chromogenic indicators (ODI, AAP/DHBS, or TMB). Again, three beads of each composition were placed into the cell (Figure SI 1) containing 1 mL of a 0.1 mM glucose solution and their color development followed capturing pictures every 5 seconds for 600 seconds. The results, summarized in Figure SI 5, showed that the behavior is dominated by the water solubility of the dyes, more so than the composition of the beads; leading to the retention of the majority of ODI (25 mg/mL) and TMB (< 1 mg/mL), but enabling a small fraction AAP/DHBS (50 mg/mL, soluble) to leach out of the beads while in contact with the solution containing the analytes (10 min). As expected, beads fabricated with 1% ALG showed the lowest retention capacity, while the ALG_{PODES} beads were superior at retaining the selected chromogenic agents, leading to the highest color intensities, and therefore supporting their use towards the development of the proposed biosensors.

These results prompted us to evaluate the storage stability of the beads. For these experiments, beads of each composition (ALG_{PODES} containing GOx/HRP and one of the chromogenic agents; ODI, AAP/DHBS, or TMB) were prepared and stored in vials either in dry form (padded on a filter paper to remove excess of water) or in wet form (immersed in 10mL of DI water). At the selected times, three beads of each composition were placed into the cell (Figure SI 1) containing 1 mL of a 0.2 mM glucose solution and their color development followed capturing pictures every 5 seconds for 60 minutes. As it can be observed in Figure 4, stable responses were obtained for all beads when stored in dry conditions. On the contrary, and in agreement with the notion that dyes can simply diffuse out of the beads following their solubility patterns, the beads stored in water produced gradually lower intensities, reaching 75% (ODI), 62% (TMB) and only 26% (AAP/DHBS) of the original response after 1 hour (Figure SI 6). While additional experiments would be required to provide a realistic estimation of the self-life of the sensors, these results allowed preparing beads for a series of experiments and keeping them (dry in a vial) without significant concerns about their activity.

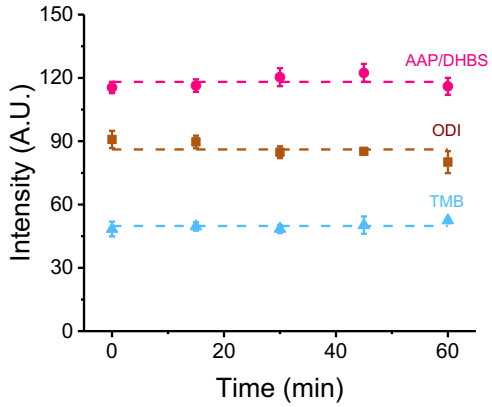

Figure 4: Retention of the dyes inside the ALG_{PODES} beads during dry storage conditions. Alginates were mixed with solutions containing o-Di, AAP/DHBS or TMB and the mixture of enzymes (GOx and HRP) in order to reach the appropriate final concentration. Beads were prepared dropping the appropriate alginate solution into 5mL of $CaCl_2$ 0.1M under constant magnetic stirring. Beads were submerged in 1mL of glucose 0.2mM.

3.3 Analysis time and sample volume. In order to determine the most appropriate analysis time, ALG_{PODES} beads were prepared with GOx/HRP (as a model reporter) but containing each of the selected chromogenic indicators (ODI, AAP/DHBS, or TMB). Again, three beads of each composition were placed into the cell containing 1 mL of a 0.1 mM glucose solution and their color development was followed capturing pictures every 5 seconds for 600 seconds. The results, summarized in Figure 5, showed a linear increase in the color intensity for all the dyes during the first minutes of the reaction, approaching a plateau after 200 sec (for AAP/DHBS) and 400 sec (for ODI). Although it was somewhat

unexpected (because the H_2O_2 generated was identical for all experiments), it was observed that the reaction with TMB did not reach a plateau during the investigated time, results than can be attributed to the short reaction time investigated (up to 10 min, while others have reported reading after 15 min[79] - 30 min[49]). In order to balance the sensitivity for the analysis using any of the dyes and considering that a small fraction of AAP/DHBS may leach out of from the beads (as previously discussed), an optimum analysis time of 300 sec was selected and used for all further analyses.

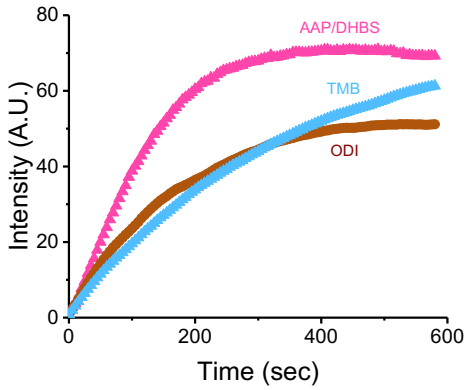

Figure 5: Signal intensity of the different dyes for ALG_{PODES} beads. Alginates were mixed with solutions containing ODI, AAP/DHBS or TMB and the mixture of enzymes (GOx and HRP) to reach the appropriate final concentration. Beads were prepared dropping the appropriate alginate solution into 5mL of $CaCl_2$ 0.1M under constant magnetic stirring. Beads were submerged in 1mL of glucose 0.1mM.

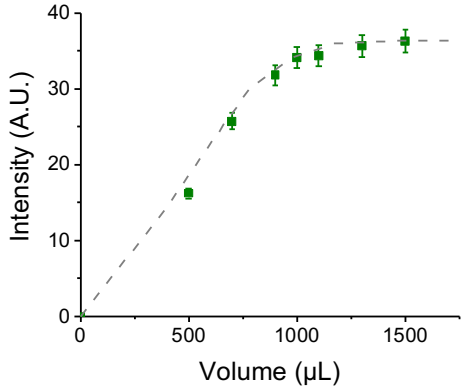

Figure 6: Signal intensity at different sample volumes. PODES was mixed with ODI dye and the mixture of enzymes (GOx and HRP) in order to reach the appropriate final concentration. Beads were prepared dropping the appropriate alginate solution into 5mL of $CaCl_2$ 0.1M under constant magnetic stirring. 0.1mM Glucose concentration.

Previous reports have described the possibility to used alginate beads as a support to trap other materials (typically hydrophobic) that act as adsorbents[7, 17-19, 80-82] and for which controlling the sample volume is essential. Considering this possibility, the color intensity of the ALG_{PODES} beads modified with GOx/HRP-ODI was investigated as a function of the sample volume, in the range between 500 µL and 1500 µL. Again, three beads were placed into the cell, the selected sample volume (containing 0.1 mM glucose) was added and then the color development was followed capturing pictures every 5 seconds for 600 seconds. As summarized in Figure 6, lower color intensities were observed when the beads were only partially immersed in the sample (< 1000 µL). Beyond that point, the beads totally submerged in the sample and the color intensity was no longer affected by the sample volume, behavior that was attributed to the hydrophilic nature of the target analyte (glucose). Considering these results, a sample volume of 1000 µL was selected as optimum and used for all remaining experiments.

3.4 Analytical performance. While there are multiple examples of smartphone-based sensors[83, 84] and biosensors,[85] one of the critical aspects that remain to be addressed is the sensitivity and practicality of these sensors towards real sample analysis. Towards that goal, the analytical performance of each of the proposed ALG$_{PODES}$ beads (modified with GOx/HRP-ODI, LOx/HRP-AAP/DHBS, or GlutOx/HRP-TMB) was determined against the corresponding target analyte and as a function of concentration. For these experiments, the ALG$_{PODES}$ beads were prepared as previously described, placed in the cell containing 1 mL of the corresponding standard solution and their color development followed with the smartphone for 5 min. Results herein reported correspond to the average and standard deviation of the color intensity obtained with at least 3 beads. As it can be observed (Figure 7) the three systems exhibited a similar, sigmoidal response with respect to the concentration, where higher concentrations of each corresponding analyte led to higher color intensities; noting that LOx/HRP-AAP/DHBS showed the best sensitivity, followed by GOx/HRP-ODI and then by GlutOx/HRP-TMB. This trend is in line with the response obtained in paper-based devices using the same enzymes/reporters[49] and can be attributed to the optical response (color intensity) of each of the chromogenic agents.

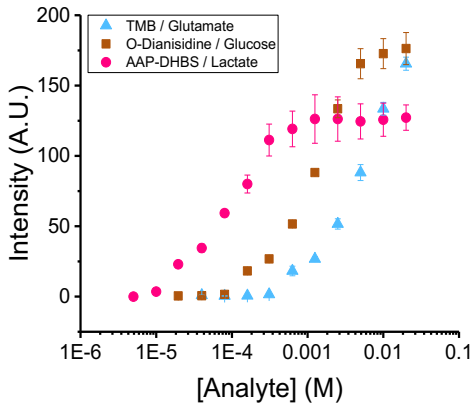

Figure 7: Calibration curves for the selected analytes. Alginates were mixed with solutions containing o-Di, AAP/DHBS or TMB and the mixture of enzymes GOx/HRP, LOx/HRP and GLOx/HRP respectively, in order to reach the appropriate final concentration. Beads were prepared dropping the appropriate alginate solution into 5mL of $CaCl_2$ 0.1M under constant magnetic stirring.

These results were used to calculate the analytical figures of merit for each enzyme/reporter, which are summarized in Table 1, where the limit of detection (LOD) and limit of quantification (LOQ) were calculated based on the standard deviation of the background noise.[86] Although these values are comparable with those recently reported in the literature (*i.e.* sub-mM LODs were reported for systems

based on TMB[87] or AAP/DHBS[88]), we believe the use of ALG_{PODES} beads represents a simpler a more practical option towards biosensing.

Table 1. Analytical performance of the three detection platforms.

	GlutOx/HRP-TMB	GOx/HRP-ODI	LOx/HRP-AAP/DHBS
Linear range	310 μM – 20.0 mM	160 μM – 20.0 mM	9.8 μM – 5.0 mM
LOD	120 μM	60 μM	6 μM
LOQ	320 μM	180 μM	19 μM

3.5 Real sample analysis. To demonstrate the applicability of the proposed ALG_{PODES} beads towards the analysis of real samples, five soy-based sauces were purchased in a local store. Besides being widely consumed around the world, these samples are produced by fermentation and naturally contain amino acids, saccharides,[89] and organic acids. In addition, they are dark in color, representing a reasonable challenge for the proposed analytical platform. Thus, the ability of the ALG_{PODES} beads to quantify glutamate, glucose, and lactate in soy sauces samples was evaluated upon a 25-fold dilution with DI water (to match the analytical range). For these experiments, the ALG_{PODES} beads were prepared as previously described, placed in the cell containing 1 mL of the corresponding standard solution and their color development followed with the smartphone for 5 min. Results herein reported correspond to the average and standard deviation of the color intensity obtained with at least 3 beads. As it can be observed in Table 2, all the samples contained different amounts of glutamate, glucose, and lactate with concentrations matching those previously reported for these sauces.[90-92]

Table 2. Results for the analysis of glutamate, glucose and lactate contained in the selected samples.

	Glutamate (mM)	Glucose (mM)	Lactate (mM)
Oyster sauce	4.5 ± 0.4	1.6 ± 0.3	0.03 ± 0.01
Orange sauce	1.27 ± 0.05	2.1 ± 0.6	0.33 ± 0.06
Low-sodium soy sauce	2.73 ± 0.02	0.85 ± 0.02	0.2 ± 0.1
Teriyaki sauce	2.4 ± 0.3	1.0 ± 0.1	0.19 ± 0.05
Soy sauce	2.4 ± 0.1	0.74 ± 0.04	0.20 ± 0.04

4. CONCLUSIONS

The present work represents the first example of a polymeric deep eutectic solvent based on alginate, compatible with stablished spherification processes (crosslinking with calcium) and supporting their application towards the development of biosensors. The formed beads displayed a narrow size distribution (2.9 ± 0.1 mm) and a permeable structure with large internal cavities (25-100 μm). These ALG_{PODES} beads were able to outperform the control beads in terms of their ability to both retain the redox dyes (small molecules) and stabilize the enzymatic reporters, aspect that was attributed to the presence of the NADES phase stabilized by hydrogen bonding. The applicability of these beads towards analytical applications (*lab-on-a-bead*) was demonstrated by integrating three sensing platforms (GlutOx/HRP-TMB, GOx/HRP-ODI, and LOx/HRP-AAP/DHBS) and by their application in real food samples. We believe the simplicity of this approach, coupled with the convenience of smartphone-base sensing, are competitive advantages with respect to other point-of-care platforms.

ACKNOWLEDGEMENTS

Authors would like to acknowledge partial financial support to this project from Clemson University, Consejo Nacional de Investigaciones Científicas y Tecnicas (CONICET) and Facultad de Ciencias Agrarias, Universidad Nacional de Cuyo (Mendoza, Argentina).

REFERENCES

1. Brostow, W.; Datashvili, T. Environmental Impact of Natural Polymers. In *Natural Polymers: Industry Techniques and Applications*, Olatunji, O. Ed.; Springer International Publishing, 2016; pp 315-338.

2. Nemani, S. K.; Annavarapu, R. K.; Mohammadian, B.; Raiyan, A.; Heil, J.; Haque, M. A.; Abdelaal, A.; Sojoudi, H. Surface Modification of Polymers: Methods and Applications. *Adv. Mater. Interfaces* **2018**, *5*, 1801247.

3. Noviana, E.; Ozer, T.; Carrell, C. S.; Link, J. S.; McMahon, C.; Jang, I.; Henry, C. S. Microfluidic Paper-Based Analytical Devices: From Design to Applications. *Chem. Rev.* **2021**, *121*, 11835-11885.

4. Silva-Neto, H. A.; Arantes, I. V. S.; Ferreira, A. L.; do Nascimento, G. H. M.; Meloni, G. N.; de Araujo, W. R.; Paixão, T. R. L. C.; Coltro, W. K. T. Recent advances on paper-based microfluidic devices for bioanalysis. *TrAC, Trends Anal. Chem.* **2023**, *158*, 116893.

5. Mabrouk, M.; Hammad, S. F.; Mansour, F. R.; Abdella, A. A. A Critical Review of Analytical Applications of Chitosan as a Sustainable Chemical with Functions Galore. *Crit Rev Anal Chem* **2022**, 1-17.

6. Dominguez, M. A.; Etcheverry, M.; Zanini, G. P. Evaluation of the adsorption kinetics of brilliant green dye onto a montmorillonite/alginate composite beads by the shrinking core model. *Adsorption* **2019**, *25*, 1387-1396.

7. Etcheverry, M.; Cappa, V.; Trelles, J.; Zanini, G. Montmorillonite-alginate beads: Natural mineral and biopolymers based sorbent of paraquat herbicides. *J. Environ. Chem. Eng.* **2017**, *5*, 5868-5875.

8. Sharma, A. K.; Priya; Kaith, B. S.; Isha; Singh, A.; Chandel, K.; Vipula. Riboflavin Functionalized Dextrin-Sodium Alginate Based Fluorescent Sensor: Detoxification of Cu2+ and Ni2+ Ions. *ACS Appl. Polym. Mater.* **2019**, *1*, 3084-3094.

9. Wen, H.; Xiao, W.; Biswas, S.; Cong, Z. Q.; Liu, X. M.; Lam, K. S.; Liao, Y. H.; Deng, W. Alginate Hydrogel Modified with a Ligand Interacting with alpha3beta1 Integrin Receptor Promotes the Differentiation of 3D Neural Spheroids toward Oligodendrocytes in Vitro. *ACS Appl Mater Interfaces* **2019**, *11*, 5821-5833.

10. Gunatilake, U. B.; Garcia-Rey, S.; Ojeda, E.; Basabe-Desmonts, L.; Benito-Lopez, F. TiO2 Nanotubes Alginate Hydrogel Scaffold for Rapid Sensing of Sweat Biomarkers: Lactate and Glucose. *ACS Appl. Polym. Mater.* **2021**, *13*, 37734-37745.

11. Aguirre Calvo, T. R.; Perullini, M.; Santagapita, P. R. Encapsulation of betacyanins and polyphenols extracted from leaves and stems of beetroot in Ca(II)-alginate beads: A structural study. *J. Food Eng.* **2018**, *235*, 32-40.

12. Maleki, G.; Woltering, E. J.; Mozafari, M. R. Applications of chitosan-based carrier as an encapsulating agent in food industry. *Trends Food Sci Technol* **2022**, *120*, 88-99.

13. Fernando, I. P. S.; Lee, W.; Han, E. J.; Ahn, G. Alginate-based nanomaterials: Fabrication techniques, properties, and applications. *Chem. Eng. J.* **2020**, *391*, 123823.

14. Teng, K.; An, Q.; Chen, Y.; Zhang, Y.; Zhao, Y. Recent Development of Alginate-Based Materials and Their Versatile Functions in Biomedicine, Flexible Electronics, and Environmental Uses. *ACS Biomaterials Science & Engineering* **2021**, *7*, 1302-1337.

15. Freitas, E. D.; Freitas, V. M. S.; Rosa, P. C. P.; da Silva, M. G. C.; Vieira, M. G. A. Development and evaluation of naproxen-loaded sericin/alginate beads for delayed and extended drug release using different covalent crosslinking agents. *Mater. Sci. Eng. C* **2021**, *118*, 111412.

16. Puiggalí-Jou, A.; Cazorla, E.; Ruano, G.; Babeli, I.; Ginebra, M.-P.; García-Torres, J.; Alemán, C. Electroresponsive Alginate-Based Hydrogels for Controlled Release of Hydrophobic Drugs. *ACS Biomaterials Science & Engineering* **2020**, *6*, 6228-6240.

17. Ehtesabi, H.; Roshani, S.; Bagheri, Z.; Yaghoubi-Avini, M. Carbon dots—Sodium alginate hydrogel: A novel tetracycline fluorescent sensor and adsorber. *J. Environ. Chem. Eng.* **2019**, *7*, 103419.

18. Van Beik, J.; Fontana, K. B.; Medeiros, D. C. C. S.; Sydney, A. C. N.; Chaves, E. S. Feasibility of calcium alginate beads to preconcentrate lead in river water samples prior to determination by flame atomic absorption spectrometry. *Environ. Monit. Assess* **2021**, *193*, 666.

19. Asghari, Z.; Sereshti, H.; Soltani, S.; Rashidi Nodeh, H.; Hossein Shojaee AliAbadi, M. Alginate aerogel beads doped with a polymeric deep eutectic solvent for green solid-phase microextraction of 5-hydroxymethylfurfural in coffee samples. *Microchem. J.* **2022**, *181*, 107729.

20. Zhuang, S.; Wang, J. Modified alginate beads as biosensor and biosorbent for simultaneous detection and removal of cobalt ions from aqueous solution. *Environ. Prog. Sustain. Energy* **2018**, *37*, 260-266.

21. Kikuchi, N.; May, M.; Zweber, M.; Madamba, J.; Stephens, C.; Kim, U.; Mobed-Miremadi, M. Sustainable, Alginate-Based Sensor for Detection of Escherichia coli in Human Breast Milk. In *Sensors*, 2020; Vol. 20.

22. Kauffman, J. S.; Ellerbrock, B. M.; Stevens, K. A.; Brown, P. J.; Pennington, W. T.; Hanks, T. W. Preparation, Characterization, and Sensing Behavior of Polydiacetylene Liposomes Embedded in Alginate Fibers. *ACS Appl. Polym. Mater.* **2009**, *1*, 1287-1291.

23. Zhang, Z.; Zhang, R.; Zou, L.; McClements, D. J. Protein encapsulation in alginate hydrogel beads: Effect of pH on microgel stability, protein retention and protein release. *Food Hydrocoll.* **2016**, *58*, 308-315.

24. Gombotz, W. R.; Wee, S. Protein release from alginate matrices. *Advanced Drug Delivery Reviews* **1998**, *31*, 267-285.

25. Voo, W.-P.; Ooi, C.-W.; Islam, A.; Tey, B.-T.; Chan, E.-S. Calcium alginate hydrogel beads with high stiffness and extended dissolution behaviour. *Eur. Polym. J.* **2016**, *75*, 343-353.

26. Liu, L.; Song, W.; Zheng, W.; Li, F.; Lv, H.; Wang, Y.; Chen, Y.; Wang, Y. Dual-responsive multilayer beads with zero leakage and controlled release triggered by near-infrared light. *Colloids Surf. B* **2022**, *220*, 112965.

27. Ramdhan, T.; Ching, S. H.; Prakash, S.; Bhandari, B. Physical and mechanical properties of alginate based composite gels. *Trends in Food Science & Technology* **2020**, *106*, 150-159.

28. Zhang, X.; Hu, B.; Zhao, Y.; Yang, Y.; Gao, Z.; Nishinari, K.; Yang, J.; Zhang, Y.; Fang, Y. Electrostatic Interaction-Based Fabrication of Calcium Alginate–Zein Core–Shell Microcapsules of Regulable Shapes and Sizes. *Langmuir* **2021**, *37*, 10424-10432.

29. Jang, S.; Son, S. U.; Kim, J.; Kim, H.; Lim, J.; Seo, S. B.; Kang, B.; Kang, T.; Jung, J.; Seo, S.; et al. Polydiacetylene-based hydrogel beads as colorimetric sensors for the detection of biogenic amines in spoiled meat. *Food Chem.* **2023**, *403*, 134317.

30. Pawar, S. N.; Edgar, K. J. Alginate derivatization: A review of chemistry, properties and applications. *Biomaterials* **2012**, *33*, 3279-3305.

31. Zhou, T.; Li, J.; Liu, P. Ionically crosslinked alginate-based nanohydrogels for tumor-specific intracellular triggered release: Effect of chemical modification. *Colloids and Surfaces A: Physicochemical and Engineering Aspects* **2018**, *553*, 180-186.

32. Polyak, B.; Geresh, S.; Marks, R. S. Synthesis and Characterization of a Biotin-Alginate Conjugate and Its Application in a Biosensor Construction. *Biomacromolecules* **2004**, *5*, 389-396.

33. Shen, K.-H.; Yeh, Y.-Y.; Chiu, T.-H.; Wang, R.; Yeh, Y.-C. Dual Dynamic Covalently Crosslinked Alginate Hydrogels with Tunable Properties and Multiple Stimuli-Responsiveness. *ACS Biomaterials Science & Engineering* **2022**, *8*, 4249-4261.

34. Yang, T.-X.; Zhao, L.-Q.; Wang, J.; Song, G.-L.; Liu, H.-M.; Cheng, H.; Yang, Z. Improving Whole-Cell Biocatalysis by Addition of Deep Eutectic Solvents and Natural Deep Eutectic Solvents. *ACS Sustainable Chemistry & Engineering* **2017**, *5*, 5713-5722.

35. Pedro, S. N.; Mendes, M. S. M.; Neves, B. M.; Almeida, I. F.; Costa, P.; Correia-Sá, I.; Vilela, C.; Freire, M. G.; Silvestre, A. J. D.; Freire, C. S. R. Deep Eutectic Solvent Formulations and Alginate-Based Hydrogels as a New Partnership for the Transdermal Administration of Anti-Inflammatory Drugs. In *Pharmaceutics*, 2022; Vol. 14.

36. Silva, J. M.; Silva, E.; Reis, R. L. Therapeutic deep eutectic solvents assisted the encapsulation of curcumin in alginate-chitosan hydrogel beads. *Sustain. Chem. Pharm.* **2021**, *24*, 100553.

37. Fernández, M. d. l. Á.; Boiteux, J.; Espino, M.; Gomez, F. J. V.; Silva, M. F. Natural deep eutectic solvents-mediated extractions: The way forward for sustainable analytical developments. *Anal. Chim. Acta* **2018**, *1038*, 1-10.

38. Lorenzetti, A. S.; Lo Fiego, M. J.; Silva, M. F.; Domini, C.; Gomez, F. J. V. Water behavior study for tailoring fructose-citric acid based natural deep eutectic solvent properties towards antibiotics solubilization. *J. Mol. Liq.* **2022**, *363*, 119917.

39. Dazat, R. E.; Vidal, E.; Lorenzetti, A. S.; García, C. D.; Domini, C.; Silva, M. F.; Gomez, F. J. V. On-Site Preparation of Natural Deep Eutectic Solvents Using Solar Energy. *ChemistrySelect* **2022**, *7*, e202104362.

40. Espino, M.; de los Ángeles Fernández, M.; Gomez, F. J. V.; Silva, M. F. Natural designer solvents for greening analytical chemistry. *TrAC, Trends Anal. Chem.* **2016**, *76*, 126-136.

41. Dazat, R. E.; Mammana, S. B.; Canizo, B. V.; Silva, M. F.; Gomez, F. J. V. Enhanced fluorescence detection of ergosterol by hydrophobic fluorescent natural deep eutectic solvent. *Green Anal. Chem.* **2022**, *3*, 100026.

42. Wei, X.; Wang, Y.; Chen, J.; Xu, P.; Xu, W.; Ni, R.; Meng, J.; Zhou, Y. Poly(deep eutectic solvent)-functionalized magnetic metal-organic framework composites coupled with solid-phase extraction for the selective separation of cationic dyes. *Anal. Chim. Acta* **2019**, *1056*, 47-61.

43. Wang, Y.; Fu, S.; Lucia, L. A.; Zhang, H. A cellulose-based self-healing composite eutectogel with reversibility and recyclability for multi-sensing. *Compos Sci Technol* **2022**, *229*, 109696.

44. Nystedt, H. L.; Grønlien, K. G.; Tønnesen, H. H. Interactions of natural deep eutectic solvents (NADES) with artificial and natural membranes. *J. Mol. Liq.* **2021**, *328*, 115452.

45. Mišan, A.; Pojić, M. Chapter Thirteen - Applications of NADES in stabilizing food and protecting food compounds against oxidation. In *Advances in Botanical Research*, Verpoorte, R., Witkamp, G.-J., Choi, Y. H. Eds.; Vol. 97; Academic Press, 2021; pp 333-359.

46. Varriale, S.; Delorme, A. E.; Andanson, J.-M.; Devemy, J.; Malfreyt, P.; Verney, V.; Pezzella, C. Enhancing the Thermostability of Engineered Laccases in Aqueous Betaine-Based Natural Deep Eutectic Solvents. *ACS Sustainable Chemistry & Engineering* **2022**, *10*, 572-581.

47. Kovács, A.; Yusupov, M.; Cornet, I.; Billen, P.; Neyts, E. C. Effect of natural deep eutectic solvents of non-eutectic compositions on enzyme stability. *Journal of Molecular Liquids* **2022**, *366*, 120180.

48. Gajardo-Parra, N. F.; Meneses, L.; Duarte, A. R. C.; Paiva, A.; Held, C. Assessing the Influence of Betaine-Based Natural Deep Eutectic Systems on Horseradish Peroxidase. *ACS Sustainable Chemistry & Engineering* **2022**, *10*, 12873-12881.

49. Evans, E.; Moreira Gabriel, E. F.; Benavidez, T. E.; Tomazelli Coltro, W. K.; Garcia, C. D. Modification of microfluidic paper-based devices with silica nanoparticles. *Analyst* **2014**, *139*, 5560-5567.

50. Reynolds, M.; Duarte, L. M.; Coltro, W. K. T.; Silva, M. F.; Gomez, F. J. V.; Garcia, C. D. Laser-engraved ammonia sensor integrating a natural deep eutectic solvent. *Microchemical Journal* **2020**, *157*, 105067.

51. Ayres, L. B.; Gomez, F. J. V.; Silva, M. F.; Linton, J. R.; Garcia, C. D. Predicting the Formation of NADES Using a Transformer-Based Model. *Sci. Rep.* **2023**, - in press.

52. Liu, Y.; Friesen, J. B.; McAlpine, J. B.; Lankin, D. C.; Chen, S.-N.; Pauli, G. F. Natural Deep Eutectic Solvents: Properties, Applications, and Perspectives. *J. Nat. Prod.* **2018**, *81*, 679-690.

53. Gawad, R.; Fellner, V. Evaluation of glycerol encapsulated with alginate and alginate-chitosan polymers in gut environment and its resistance to rumen microbial degradation. *Asian-Australas J Anim Sci* **2019**, *32*, 72-81.

54. Kim, J.; Hiltpold, I.; Jaffuel, G.; Sbaiti, I.; Hibbard, B. E.; Turlings, T. C. J. Calcium-alginate beads as a formulation for the application of entomopathogenic nematodes to control rootworms. *J Pest Sci* **2021**, *94*, 1197-1208.

55. Gabriel, E. F. M.; Coltro, W. K. T.; Garcia, C. D. Fast and versatile fabrication of PMMA microchip electrophoretic devices by laser engraving. *Electrophoresis* **2014**, *35*, 2325-2332.

56. Schneider, C. A.; Rasband, W. S.; Eliceiri, K. W. NIH Image to ImageJ: 25 years of image analysis. *Nat. Methods* **2012**, *9*, 671-675.

57. Chan, E.-S.; Wong, S.-L.; Lee, P.-P.; Lee, J.-S.; Ti, T. B.; Zhang, Z.; Poncelet, D.; Ravindra, P.; Phan, S.-H.; Yim, Z.-H. Effects of starch filler on the physical properties of lyophilized calcium–alginate beads and the viability of encapsulated cells. *Carbohydr. Polym.* **2011**, *83*, 225-232.

58. Chen, Y.; Wu, Q.; Zhang, Z.; Yuan, L.; Liu, X.; Zhou, L. Preparation of Curcumin-Loaded Liposomes and Evaluation of Their Skin Permeation and Pharmacodynamics. *Molecules* **2012**, *17*, 5972-5987.

59. Jeong, C.; Kim, S.; Lee, C.; Cho, S.; Kim, S.-B. Changes in the Physical Properties of Calcium Alginate Gel Beads under a Wide Range of Gelation Temperature Conditions. *Foods* **2020**, *9*, 180.

60. Chan, E.-S.; Lee, B.-B.; Ravindra, P.; Poncelet, D. Prediction models for shape and size of ca-alginate macrobeads produced through extrusion–dripping method. *J Colloid Interface Sci* **2009**, *338*, 63-72.

61. Lee, B. B.; Ravindra, P.; Chan, E. S. Size and Shape of Calcium Alginate Beads Produced by Extrusion Dripping. *Chem Eng Technol* **2013**, *36*, 1627-1642.

62. Davarcı, F.; Turan, D.; Ozcelik, B.; Poncelet, D. The influence of solution viscosities and surface tension on calcium-alginate microbead formation using dripping technique. *Food Hydrocoll.* **2017**, *62*, 119-127.

63. Bennacef, C.; Desobry-Banon, S.; Probst, L.; Desobry, S. Advances on alginate use for spherification to encapsulate biomolecules. *Food Hydrocoll.* **2021**, *118*, 106782.

64. Lores, H.; Romero, V.; Costas, I.; Bendicho, C.; Lavilla, I. Natural deep eutectic solvents in combination with ultrasonic energy as a green approach for solubilisation of proteins: application to gluten determination by immunoassay. *Talanta* **2017**, *162*, 453-459.

65. Ling, J. K. U.; Hadinoto, K. Deep Eutectic Solvent as Green Solvent in Extraction of Biological Macromolecules: A Review. *Int. J. Mol. Sci.* **2022**, *23*, 3381.

66. Durán, G. M.; Benavidez, T. E.; Ríos, Á.; García, C. D. Quantum dot-modified paper-based assay for glucose screening. *Microchim. Acta* **2016**, *183*, 611-616.

67. Onda, M.; Ariga, K.; Kunitake, T. Activity and stability of glucose oxidase in molecular films assembled alternately with polyions. *J. Biosci. Bioeng.* **1999**, *87*, 69-75.

68. Nejadnik, M. R.; Deepak , F. L.; Garcia, C. D. Adsorption of Glucose Oxidase to 3-D Scaffolds of Carbon Nanotubes: Analytical Applications. *Electroanalysis* **2011**, *23*, 1462-1469.

69. Yoo, S.; Min, K.; Tae, G.; Han, M. S. A long-term stable paper-based glucose sensor using a glucose oxidase-loaded, Mn2BPMP-conjugated nanocarrier with a smartphone readout. *Nanoscale* **2021**, *13*, 4467-4474.

70. Márquez, A.; Jiménez-Jorquera, C.; Domínguez, C.; Muñoz-Berbel, X. Electrodepositable alginate membranes for enzymatic sensors: An amperometric glucose biosensor for whole blood analysis. *Biosens. Bioelectron.* **2017**, *97*, 136-142.

71. Fu, J.-J.; Sun, C.; Xu, X.-B.; Zhou, D.-Y.; Song, L.; Zhu, B.-W. Improving the functional properties of bovine serum albumin-glucose conjugates in natural deep eutectic solvents. *Food Chem.* **2020**, *328*, 127122.

72. Pal, S.; Roy, R.; Paul, S. Potential of a Natural Deep Eutectic Solvent, Glyceline, in the Thermal Stability of the Trp-Cage Mini-protein. *J. Phys. Chem. B.* **2020**, *124*, 7598-7610.

73. Liu, Y.; Wang, Y.; Dai, Q.; Zhou, Y. Magnetic deep eutectic solvents molecularly imprinted polymers for the selective recognition and separation of protein. *Anal. Chim. Acta* **2016**, *936*, 168-178.

74. Roda, A.; Matias, A. A.; Paiva, A.; Duarte, A. R. C. Polymer Science and Engineering Using Deep Eutectic Solvents. *Polymers* **2019**, *11*, 912.

75. Dabhade, A.; Jayaraman, S.; Paramasivan, B. Development of glucose oxidase-chitosan immobilized paper biosensor using screen-printed electrode for amperometric detection of Cr(VI) in water. *3 Biotech* **2021**, *11*, 183.

76. Zhai, P.; Chen, X. B.; Schreyer, D. J. PLGA/alginate composite microspheres for hydrophilic protein delivery. *Mater. Sci. Eng. C* **2015**, *56*, 251-259.

77. Kopač, T.; Krajnc, M.; Ručigaj, A. Protein release from nanocellulose and alginate hydrogels: The study of adsorption and desorption kinetics. *Colloids Surf. B* **2022**, *217*, 112677.

78. Liu, H.; Chiou, B.-S.; Ma, Y.; Corke, H.; Liu, F. Reducing synthetic colorants release from alginate-based liquid-core beads with a zein shell. *Food Chem.* **2022**, *384*, 132493.

79. Gabriel, E. F.; Garcia, P. T.; Lopes, F. M.; Coltro, W. K. Paper-Based Colorimetric Biosensor for Tear Glucose Measurements. In *Micromachines*, 2017; Vol. 8.

80. Asthana, A.; Verma, R.; Singh, A. K.; Susan, M. A. B. H.; Adhikari, R. Silver Nanoparticle Entrapped Calcium-Alginate Beads for Fe(II) Removal via Adsorption. *Macromol. Symp.* **2016**, *366*, 42-51.

81. Tasmia; Shah, J.; Jan, M. R. Eco-friendly alginate encapsulated magnetic graphene oxide beads for solid phase microextraction of endocrine disrupting compounds from water samples. *Ecotoxicol. Environ. Saf.* **2020**, *190*, 110099.

82. Hamadan, R.; Al-Taee, M. M.; Mahdi, A. B.; Hadrawi, S. K.; Dwijendra, N. K. A.; Kavitha, M.; Mustafa, Y. F.; Wadday, A. K. Entrapment of polyethylene terephthalate derived carbon in Ca-alginate beads for solid phase extraction of polycyclic aromatic hydrocarbons from environmental water samples. *Inorg. Chem. Commun.* **2022**, *146*, 110147.

83. Ayres, L. B.; Lopes, F. S.; Garcia, C. D.; Gutz, I. G. R. Integrated instrumental analysis teaching platform with smartphone-operated fluorometer. *Anal. Methods* **2020**, *12*, 4109-4115.

84. Vidal, E.; Lorenzetti, A. S.; Garcia, C. D.; Domini, C. E. Use of universal 3D-Printed smartphone spectrophotometer to develop a time-based analysis for hypochlorite. *Anal. Chim. Acta* **2021**, *1151*, 338249.

85. Qian, S.; Cui, Y.; Cai, Z.; Li, L. Applications of smartphone-based colorimetric biosensors. *Biosens. Bioelectron. X* **2022**, *11*, 100173.

86. Fernandez-Ramos, M. D.; Cuadros-Rodriguez, L.; Arroyo-Guerrero, E.; Capitan-Vallvey, L. F. An IUPAC-based approach to estimate the detection limit in co-extraction-based optical sensors for anions with sigmoidal response calibration curves. *Anal Bioanal Chem* **2011**, *401*, 2881-2889.

87. Yüzer, E.; Doğan, V.; Kılıç, V.; Şen, M. Smartphone embedded deep learning approach for highly accurate and automated colorimetric lactate analysis in sweat. *Sens. Actuators B Chem.* **2022**, *371*, 132489.

88. Kim, S.; Kim, D.; Kim, S. Simultaneous quantification of multiple biomarkers on a self-calibrating microfluidic paper-based analytic device. *Anal. Chim. Acta* **2020**, *1097*, 120-126.

89. Katayama, H.; Tatemichi, Y.; Nakajima, A. Simultaneous quantification of twenty Amadori products in soy sauce using liquid chromatography-tandem mass spectrometry. *Food Chem.* **2017**, *228*, 279-286.

90. Artigues, M.; Abellà, J.; Colominas, S. Analytical Parameters of an Amperometric Glucose Biosensor for Fast Analysis in Food Samples. *Sensors* **2017**, *17*, 2620.

91. Udomsopagit, S.; Suphantharika, M.; Künnecke, W.; Bilitewski, U.; Bhumiratana, A. Determination of l-glutamate in various commercial soy sauce products using flow injection analysis with a modified electrode. *World J. Microbiol. Biotechnol.* **1998**, *14*, 543-549.

92. Kanbe, C.; Ozawa, Y.; Sakasai, T. Automated Measurement of d(−), l(+)-Lactate in Soy Sauce and Wine. *Agric. Biol. Chem.* **1977**, *41*, 863-867.